

Tunnel-Diode Low-Level Detection

WILLIAM F. GABRIEL, SENIOR MEMBER, IEEE

Abstract—An analysis of tunnel-diode low-level detection is presented for the purpose of explaining some of the unusual detection characteristics that occur under certain bias conditions. For example, in the vicinity of its inflection bias point, a tunnel diode exhibits a discriminator-like rectification behavior with two sensitivity peaks. When biased at one of these peaks, the diode is capable of unusually high sensitivities, at least an order of magnitude better than the sensitivity of any other known diode. It is shown that these high sensitivities are proportional to $(1 - \Gamma^2)$, where Γ^2 is the RF power gain of the detector viewed as a reflection-type amplifier. The resultant gain bandwidth (or sensitivity bandwidth) limitations of the detector are discussed. Unusually high sensitivities are also possible at the lower microwave frequencies when the tunnel diode is biased at its peak current point.

A knowledge of the diode static characteristics, the reflection coefficient, and the video circuit permits an accurate analytical evaluation of the sensitivity performance of any tunnel diode, and calculations are carried out for an example diode and compared against measured data. The paper also contains a specific comparison of the relative sensitivity performance of the example tunnel diode versus a hot carrier diode.

I. INTRODUCTION

MICROWAVE low-level detection, which was entirely dependent upon the rather unpredictable silicon point-contact crystal rectifier^[1] for so many years, has been advanced considerably by the development of tunnel-diode (or back-diode) detectors and hot carrier-diode detectors. Both of these solid junction devices have demonstrated advantages of lower noise [particularly $1/f$ (flicker) noise], higher rectification current sensitivity, low temperature variation, high burn-out capability, high resistance to noise impulse generation under shock and vibration, aging stability, broad bandwidth capability, and accurate analytical performance evaluation from measured static characteristics.

The excellent performance of the hot carrier diode under bias conditions has been reported in Hall^[2] and Sorensen^[3] together with an adequate analysis. In the case of the tunnel diode, however, despite numerous references^{[4]–[10]} reporting on specific examples of sensitivity performance, the analyses are found to be restricted and incomplete such that important features of the overall behavior of this versatile detector are overlooked. For instance, it is not generally appreciated that the tunnel diode, when biased in its negative resistance region, is capable of at least an order of magnitude of greater sensitivity than any other diode detector for frequencies below resistive cutoff; also, that it is capable of bipolar amplitude modulation of its video output. The former

capability can be of considerable advantage in sensitive TRF (tuned radio frequency) receivers^{[11],[12]} such as those employed in compact solid-state transponders for missiles, spacecraft, and aircraft.

The purpose of this paper is to present a low-level detector analysis which is general enough to cover tunnel-diode behavior for any bias condition, and to demonstrate detection features which are peculiar to the tunnel diode. Super regenerative detection and converter action are not included in this discussion, i.e., the tunnel-diode detector circuit is assumed to be in a stable condition at all times.

In the work described herein, the rectification current sensitivity β is expressed as a function of the reflection coefficient Γ and it is shown that a knowledge of this quantity, together with the diode static characteristics and the video circuit, permits accurate analysis of low-level detection performance for any bias condition. Calculations are carried through on an example diode and compared against measured data.

When a tunnel-diode detector is biased in its negative resistance region and operated below resistive cutoff frequency, it is an RF amplifier and must look into an impedance that insures stable operation, i.e., it requires a nonreciprocal isolator or circulator to insure stability against spurious oscillations. Also, as an amplifier it exhibits the usual gain bandwidth limitations, and examples of sensitivity behavior versus RF bandwidth are discussed.

The final section of the paper discusses the diode figure of merit M and here a specific comparison with the hot carrier diode is made in order to illustrate relative sensitivity capability.

II. EQUIVALENT CIRCUIT AND DIODE CHARACTERISTICS

Microwave low-level detectors usually consist of a combination of transmission-line circuits and lumped reactances, plus the diode. The complete detailed equivalent circuit can be quite complicated, particularly in the case of broadband designs, but for the purposes of the present analytical discussion it is preferable to reduce down to the simple equivalent circuit shown in Fig. 1. This circuit is referenced to the diode junction and is often utilized for diode analysis.^{[13]–[17]} Circuit elements R_g and L are both functions of frequency since they represent the series equivalent of the impedance that includes the diode series inductance, the diode package capacitance, and the entire external RF input circuit.

The differential junction resistance R may assume either positive or negative values. When it is negative, the circuit represents a negative-resistance reflection-type amplifier where the voltage gain is simply equal to the reflection coefficient Γ referred to R_g , i.e.,

Manuscript received October 25, 1966; revised May 22, 1967. This paper is based on NASA Tech. Note D-3905, June, 1967 while the author was at NASA-Goddard Space Flight Center, Greenbelt, Md.

The author is presently with Scanwell Laboratories, Inc., Springfield, Va.

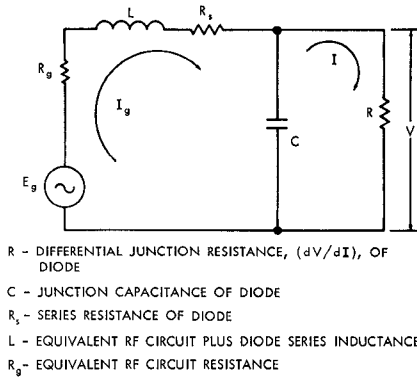


Fig. 1. Equivalent circuit of detector referred to diode junction.

$$\Gamma = \frac{(Z - R_g) - R_g}{(Z - R_g) + R_g} = \frac{Z - 2R_g}{Z}, \quad (1)$$

where Z is the total series impedance of the circuit.

$$Z = \left[R_g + R_s + \frac{R}{1 + (\omega CR)^2} \right] + j \left[\omega L - \frac{R(\omega CR)}{1 + (\omega CR)^2} \right]. \quad (2)$$

This type of tunnel-diode amplifier and its stability considerations are widely discussed in the literature.^{[13]-[21]} Circuit stability criteria must be satisfied at all frequencies below the resistive cutoff frequency in order to insure finite values for Γ and avoid spurious oscillations. For Fig. 1, a safe and sufficient^[18] stability criterion¹ may be written in the form

$$|R| > (R_s + R_g) > \frac{L}{|R|C} \quad \text{for negative } R. \quad (3)$$

A small signal analysis of the Fig. 1 circuit is carried out in Appendix I for the purpose of deriving a general expression for β , and there it is shown that the basic diode quantities required are G , R_s , C , and G' , where G' is the first derivative of the diode differential junction conductance, G . For purposes of practical illustration and experimental confirmation, the measured characteristics of an actual diode example, a selected commercial MS1012 back diode, will be utilized throughout the discussion.

A back diode^[21] is simply a tunnel diode with a low peak current wherein the "forward voltage" direction is reversed (backwards) from the usual tunnel-diode polarity. Fig. 2 illustrates the V - I characteristic of the example diode and, also, a typical hot carrier diode. Three distinct bias points are denoted on the back diode curve because they are often referred to and used as subscripts on the voltage and current:

- 0 refers to the zero bias point,
- p refers to the peak current bias point, and
- i refers to the inflection bias point.

Although the low peak current ($I_p = -0.286$ mA) qualifies the example diode to be called a back diode, it will be referred to as a tunnel diode because it has a resistive cutoff frequency of about 9 GHz and, also, it was chosen specifically to demonstrate the detection behavior that can be obtained when biased into the negative resistance region.

A calculation of the derivatives, G and G' , from Fig. 2 requires an analytical expression for the tunnel-diode current. This problem is treated in Appendix II, and the results are plotted in Fig. 3 for the diode voltage range of greatest interest. It will be noted that the voltage scale in Fig. 3 is the diode junction voltage instead of the diode bias voltage, i.e.,

$$V_b = V + IR_s, \quad (4)$$

where V is the internal junction voltage and V_b is the external bias voltage across the diode terminals. The junction voltage is required for the calculations. G and G' for a tunnel diode behave in a manner different than the similar derivatives of a hot carrier or point contact diode in that they do not bear a constant ratio to one another; they both have a zero point and they both can assume negative values as well as positive values.

The diode series resistance R_s can be found from the forward conduction characteristic (a standard technique) as described in Appendix II, if it is not given as part of the manufacturer's data. A value of 8 ohms for R_s was measured on the example diode with an estimated accuracy of 5 percent.

Diode junction capacitance C must also be measured if not given by the manufacturer. Applicable measurement techniques include the familiar RF bridge method,^[22] microwave impedance determination, or resistive cutoff frequency determination. For the example diode, the latter approach was employed. The resistive cutoff frequency f_r occurs at the point where the equivalent series resistance of the diode goes to zero, and it is readily shown that

$$f_r = \frac{\sqrt{\frac{|R|}{R_s} - 1}}{2\pi C |R|} \quad \text{for negative } R. \quad (5)$$

Since the total series resistance is zero at f_r , it follows that the diode will look like a short circuit at resonance whereby $\Gamma = -1$. Thus, the technique consists of tuning the detector to resonance at any convenient microwave frequency, and recording the bias voltage required to give a reflection coefficient exactly equal to unity at that frequency. The frequency thereby becomes an f_r value; R_s is known; R can be determined from Fig. 3(b) since the bias voltage is known; and this then permits solving for C from (5). A value of 0.3 pF was arrived at for the example diode via this technique.

The f_r technique is easy to implement and use, and it has a great advantage in that it is independent of the diode package capacitance.

¹ In addition to the RF circuit, the detector video circuit and dc bias circuit must also satisfy their stability criteria.

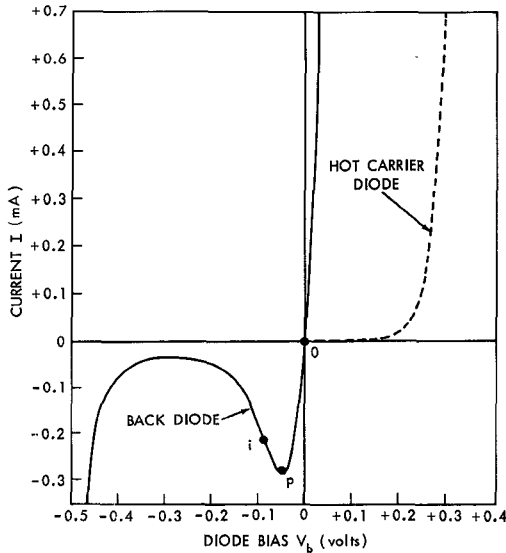


Fig. 2. Static voltage-current characteristics for example diode (MS1012) and a hot carrier diode (hpa-2350) at 25°C.

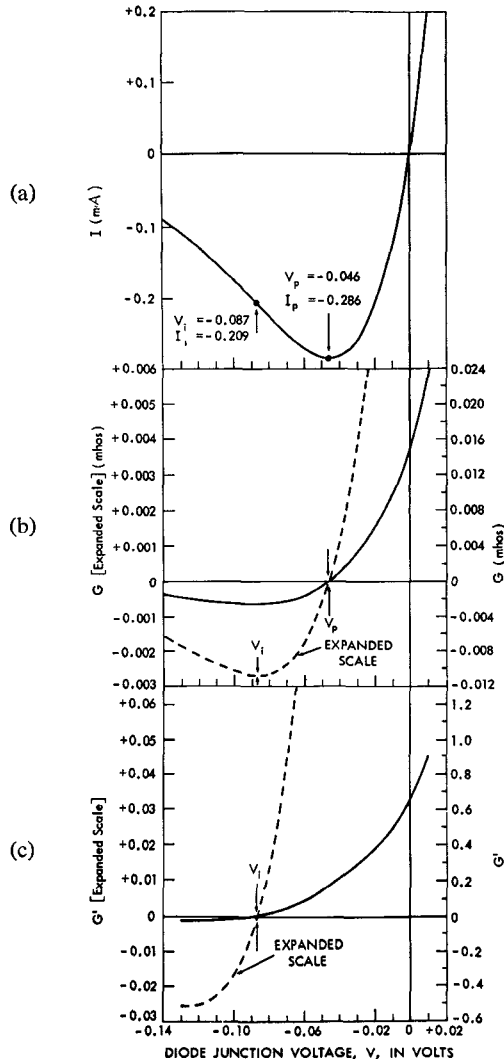


Fig. 3. Static characteristics versus diode junction voltage V . (a) Current I versus V . (b) Differential junction conductance G versus V . (c) First derivative of G , G' versus V .

III. RECTIFICATION CURRENT SENSITIVITY β

The rectification current sensitivity β is defined as the ratio of the detector rectified output current I_r to the RF power P_i incident upon the detector, or

$$I_r = \beta P_i. \quad (6)$$

A general equation for β is derived in Appendix I on the basis of a small signal analysis of the detector equivalent circuit shown in Fig. 1

$$\beta = \frac{2G'R_g |Z_j|^2}{(1 + GR_s) |Z|^2} \quad (7)$$

where

$$Z_j = \frac{1}{G + j\omega C} \quad (8)$$

and Z is given by (2). Equation (7) holds for either positive or negative values of G , subject to the restriction that the tunnel-diode circuit be stable. An inspection of the various terms in (7) shows that β will vary principally as a function of three parameters:

- 1) diode bias voltage,
- 2) equivalent source resistance R_g , and
- 3) frequency.

A variation in the diode bias voltage causes a variation in G and G' as illustrated by Fig. 3. Junction capacitance C also changes with bias,^[15] but the effect is of minor importance compared to G and G' .

R_g determines the reflection coefficient Γ as given by (1).² Because of the familiar interpretation of Γ for tunnel diodes and the fact that it is a readily measured microwave quantity, it becomes desirable to convert the series impedance Z in (7) to Γ . Solving for Z from (1) results in

$$Z = \left(\frac{2R_g}{1 - \Gamma} \right) \quad (9)$$

and substituting this into (7) permits β to be written as

$$\beta = \frac{G' |1 - \Gamma|^2}{2R_g(1 + GR_s)(G^2 + (\omega C)^2)}. \quad (10)$$

It will be noted that β can increase almost in direct proportion to the RF power gain $|\Gamma|^2$ of the tunnel diode, thus indicating the possibility of very large current sensitivities

Equation (10) can be manipulated into several interesting forms by applying appropriate restrictions upon Γ and G . If we apply the restriction that Γ be real (circuit resonance condition), then from (2) and (1)

$$Z = R_g + R_s + r \quad (11)$$

² This interpretation is dependent upon R_g representing only the generator source resistance. If R_g includes any loss components then (1) and (7) must be corrected to incorporate the loss factor.

and

$$\Gamma = \frac{R_s + r - R_g}{R_s + r + R_g} \quad (12)$$

where

$$r = \frac{R}{1 + (\omega CR)^2} \quad (13)$$

The value r is the equivalent series resistance of the diode junction. Solving for R_g from (12) and substituting into (10) results in

$$\beta_1 = \beta_0 \left[\frac{1 - \Gamma^2}{1 + \left(\frac{R_s(\omega CR)^2}{R + R_s} \right)} \right] \quad \text{restrictions: } \Gamma \text{ is real} \quad (14)$$

where

$$\beta_0 = \frac{G'}{2G(1 + GR_s)^2} \quad (15)$$

If we next restrict G to positive values only, then (14) may be written as

$$\beta_2 = \beta_0 \left[\frac{1 - \Gamma^2}{1 + \left(\frac{f}{f_c} \right)^2} \right] \quad \begin{array}{l} \text{restrictions: } \Gamma \text{ is real,} \\ G \text{ is positive} \end{array} \quad (16)$$

where

$$f_c = \frac{\sqrt{\left(\frac{R}{R_s} \right) + 1}}{2\pi CR} \quad (17)$$

Equation (16) applies to hot carrier and point contact diodes as well as tunnel diodes. The frequency f_c is the usual "cutoff" frequency defined for diodes. For a positive G , $|\Gamma| \leq 1$ so that the optimum value of β_2 occurs for matched conditions, i.e., $\Gamma=0$, whereupon (16) becomes identical to the usual current sensitivity expressions found in Torrey and Whitmer^[1] and Sorensen.^[2]

A special form for β occurs when we impose the restriction of biasing the tunnel diode at its peak current point (I_p , V_p) where G goes to zero. From (9) through (11) one obtains the simple expression

$$\beta_p = \frac{G'(1 - \Gamma^2)}{2R_s(\omega C)^2} \quad \begin{array}{l} \text{restrictions: } \Gamma \text{ is real,} \\ G \text{ is zero.} \end{array} \quad (18)$$

Like β_2 above, β_p is optimized for $\Gamma=0$.

If we restrict G to negative values only, then (14) may be written as

$$\beta_3 = \beta_0 \left[\frac{1 - \Gamma^2}{1 - \left(\frac{f}{f_r} \right)^2} \right] \quad \begin{array}{l} \text{restrictions: } \Gamma \text{ is real,} \\ G \text{ is negative} \end{array} \quad (19)$$

where

$$f_r = \frac{\sqrt{\frac{|R|}{R_s} - 1}}{2\pi C|R|} \quad (20)$$

The frequency f_r will be recognized as the resistive cutoff frequency of a tunnel diode, above which the diode cannot supply RF gain, i.e., $|\Gamma| < 1$ for $f > f_r$. It follows that for $f > f_r$, β_3 will be optimized when $\Gamma=0$.

When $f=f_r$, the β_3 expression becomes indeterminate and one must go back to the general equation (10) to compute β , utilizing the fact that $\Gamma=-1$ for this particular condition.

Finally, when $f < f_r$, then from (12) we see that $|\Gamma| > 1$ and may be made arbitrarily large by adjusting R_g , so that no optimum value for β_3 can be defined and it may be increased without limit, at least in theory.

A plot of the two frequencies f_c and f_r versus bias for the example tunnel diode is shown in Fig. 4. Knowing these values, it is then a simple matter to compute the gross frequency behavior of β from (16) or (19) for a given Γ . The data points shown in Fig. 4 were the frequencies at which f_r measurements were made in order to determine the value of the diode junction capacitance (refer to Section III for description of measurement).

Fig. 5 illustrates the gross frequency behavior of β for the example diode under various bias conditions and specified values of Γ . The optimum curves for zero bias $V=-0.02$ volts and $V=-0.04$ volts are calculated from (16) since G is positive. The zero bias curve shows good sensitivity capability in the millimeter-wave frequency region.

The optimum curve for the peak current bias point, $V_p=-0.046$ volts, is calculated from (18) since G is zero, and it demonstrates the unique 6 dB per octave constant slope obtained for this particular bias condition. Note that this constant slope behavior results in unusually high sensitivities at the lower microwave frequencies, and full advantage may be taken of this if the circuit losses can be kept small, i.e., the detector circuit Q is inversely proportional to frequency ($Q=1/2\omega CR_s$) for the V_p bias condition.

The dashed line curve for $V=-0.07$ volts, $\Gamma=-10$, $f < f_r$ is calculated from (19) since G is negative, and it clearly shows the high sensitivities that can be obtained at microwave frequencies below resistive cutoff when a tunnel diode is biased in its negative resistance region. An interesting feature of this curve is that β tends to approach infinity as the frequency approaches f_r . This behavior is simply the result of assuming a constant value for Γ , whereby the circuit Q would increase rapidly as f_r was approached. In actual practice, operation close to f_r requires such low generator impedances to maintain a given value of Γ that coupling circuit losses become important and the resultant attenuation of the incident RF power must be taken into account.

The importance of f_r in tunnel-diode detection cannot be emphasized too strongly, because detection sensitivity drops rather abruptly beyond f_r and results in poor sensitivity performance. This behavior is illustrated by the dashed-line optimum curve for $V=-0.07$ volts, $f > f_r$ which

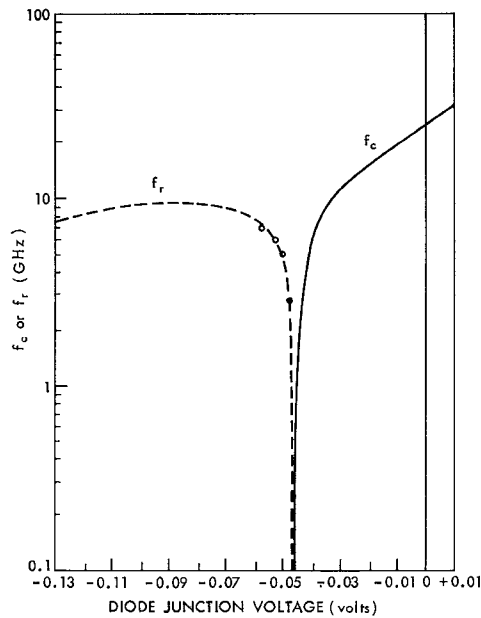


Fig. 4. f_c and f_r versus junction voltage for example diode.

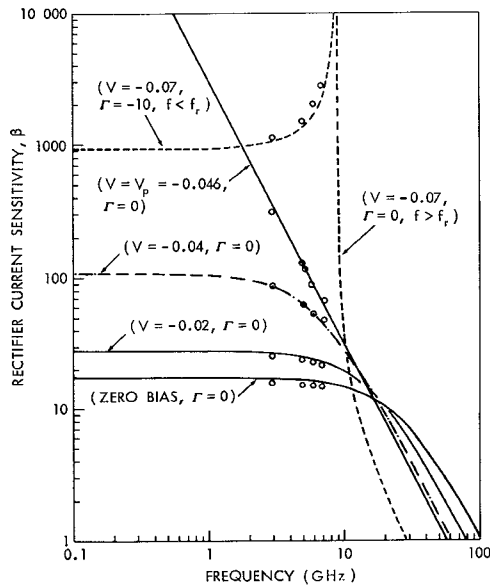


Fig. 5. Gross frequency behavior of β for example diode at various bias conditions and specified values of Γ .

is also calculated from (19). Note that this curve drops below the zero bias curve by a factor of about ten in the millimeter-wave region.

The calculated curves of Fig. 5 have been experimentally verified for the example diode at spot frequencies of 3, 5, 6, and 7 GHz, as illustrated by the data points plotted thereon. Experimental confirmation at many other values of Γ was obtained, but the data has been omitted in the interest of keeping the family of curves as simple as possible.

From Fig. 5 it is evident that there must be a continuous variation in β versus bias under stable operating conditions, and a typical example of this type of variation is illustrated in Fig. 6(a) for the example diode. The solid curve was calculated from (10) under the conditions of $R_g = 85$ ohms

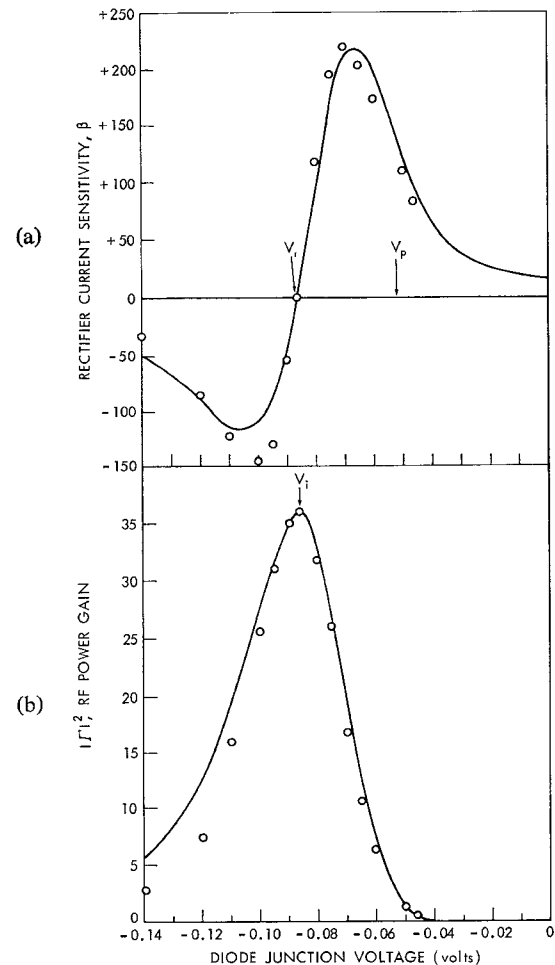


Fig. 6. β and $|\Gamma|^2$ versus junction voltage for example diode under conditions of $R_g = 85$ ohms and detector circuit resonance at 3 GHz. (a) β versus diode junction voltage. (b) $|\Gamma|^2$ versus diode junction voltage.

and detector circuit resonance at 3 GHz. Note the bipolar behavior of β caused by the change in sign of G' as the diode is biased through the inflection point (see Fig. 3). The tunnel diode changes its direction of rectification when biased beyond the inflection point. Fig. 6(b) illustrates the associated variation in $|\Gamma|^2$ versus bias, which demonstrates the fact that rectification passes through zero at the peak RF gain point (under single-tuned conditions). This rectification reversal results in a discriminator-like characteristic with two sensitivity peaks, one above and one below the inflection bias point. The upper peak point has the highest sensitivity and is generally utilized as the operating bias point for high-sensitivity detectors.

The discriminator-like characteristic can be utilized for bipolar amplitude modulation of output video signals via bias voltage control. This property would be useful, for example, in feedback control of tunnel-diode amplifier operating bias point.

Experimental data points measured at 3 GHz for the assumed conditions are also shown plotted in Fig. 6(a) and Fig. 6(b). The equivalent generator impedance of 85 ohms was initially approximated by adjusting the detector for an

RF power gain of 15.6 dB (calculated from (12) for $R_g=85$ ohms) with the diode biased at its inflection point. The discrepancies between the measured data and calculated curves appear reasonable in view of the R_g approximation plus expected error in the values of G , G' , and C .

As a practical note, it might be pointed out that the zero rectification point provides an extremely sensitive means for locating the exact inflection point on a tunnel-diode characteristic.

IV. BANDWIDTH BEHAVIOR OF β

In general, bandwidth will be inversely proportional to the Q factor of the equivalent circuit shown in Fig. 1, which may be written

$$Q = \left(\frac{\omega_0 L}{R_g + R_s + r_0} \right) \tag{21}$$

where

$$r_0 = \frac{R}{1 + (\omega_0 CR)^2} \tag{22}$$

ω_0 is taken to be the center frequency of the passband and r_0 is the equivalent series resistance of the diode junction at ω_0 . For purposes of illustration, it is convenient to calculate the simple case of fixed-element single-tuned series resonance³ wherein the bandwidth Δf is given by the familiar ratio of f_0/Q , so that from (21) one obtains

$$\Delta f = \frac{f_0}{Q} = \frac{R_g + R_s + r_0}{2\pi L} \tag{23}$$

Upon substituting for L from the single-tuned resonance condition

$$\omega_0 L = r_0(\omega_0 CR) \tag{24}$$

and expressing R_g in terms of reflection coefficient Γ_0 , (23) may be manipulated into the form

$$\Delta f = \frac{1 + \left(\frac{R_s}{r_0} \right)}{\pi RC(1 + \Gamma_0)} \tag{25}$$

An inspection of (25) shows that bandwidth becomes inversely proportional to the RF voltage gain of the tunnel-diode circuit. Also, the maximum gain bandwidth product is equal to $(1/\pi RC)$, which is in agreement with derivations contained in Hines^[13] for the single-tuned circuit case.

Fig. 7 illustrates a plot of β versus bandwidth, with values of Δf calculated from (25) for the example diode under conditions of $V=-0.07$ volts and circuit resonance at 6 GHz. Fig. 7 also contains a plot of β versus bandwidth as measured on the tuned detector mount that was utilized for obtaining the experimental C-band data. This particular

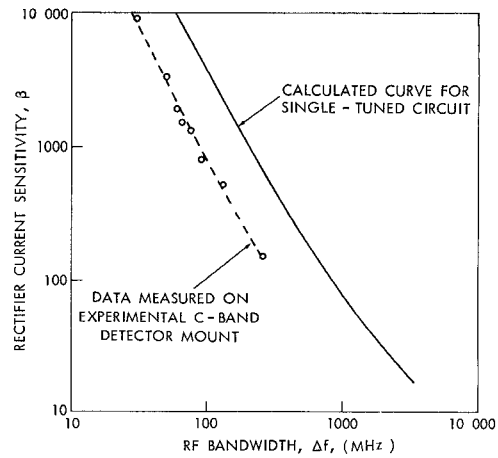


Fig. 7. β versus RF bandwidth for example diode under conditions $V=-0.07$ volts and circuit resonance at 6 GHz. The calculated curve assumes that R_g , L , and r_0 are frequency independent.

detector mount design did not have a bandwidth performance equal to that of a fixed-element single-tuned circuit because of the variation of R_g and L with frequency. Note the characteristic slope of approximately 6 dB per octave in β versus Δf .

Bandwidth performance is always dependent upon the particular circuits that are utilized in coupling the generator source to the diode. In the extensive literature that exists on the gain bandwidth products of amplifiers,^{[23]-[32]} Matthaei^[23] and others have pointed out that considerable bandwidth improvements may be obtained through proper design of more complex impedance transformation circuits between the generator source and the diode.

V. NOISE OF TUNNEL DIODE AND VIDEO CIRCUIT

From the standpoint of low-level video detection, one of the most important characteristics of the tunnel diode is its low $1/f$ (flicker) noise. Investigators^{[4], [33], [34]} have found that the $1/f$ noise corner frequency is on the order of 1 kHz when the diodes are operated in the low-voltage positive-conductance region. In fact, for this bias region the tunnel diode (or back diode) has a low-noise performance comparable to the hot carrier diode.^[3] When biased to the peak current point and beyond into the negative resistance region, the $1/f$ noise corner frequency increases steadily^{[22], [34]-[37]} and can deteriorate markedly as the valley region is approached, apparently because of the very noisy character of the valley region excess current. Valley region excess video noise varies from one diode to another,^[34] but it is generally always high enough that this region of operation should be avoided for high-sensitivity applications. Therefore, the present video noise discussion will proceed on the assumption that the tunnel-diode bias voltage excursion shall avoid entering the valley region in order that $1/f$ noise may remain reasonably small.⁴

³ It is assumed that the reader recognizes the fact that the circuit of Fig. 1 is not actually a fixed-element single-tuned circuit because of frequency dependence in R_g , L , and r .

⁴ Obviously, if the "video bandwidth" upper frequency limit happens to be in the kilohertz range of frequencies, then the $1/f$ noise may not be negligible and its contribution must be accounted for.

If $1/f$ noise is neglected, then the diode video noise can be attributed to shot noise and thermal noise components which have been shown^{[17], [38], [39]} to be represented by the equivalent circuit of Fig. 8(a), where e_n^2 and i_n^2 are given by

$$e_n^2 = 4KT B_v R_s \quad (26)$$

and

$$i_n^2 = 2qI_{eq} B_v \quad (27)$$

where

B_v = video noise bandwidth,

$q = 1.6 \cdot 10^{-19}$ coulombs,

I_{eq} = equivalent shot-noise-producing dc current, and

K = Boltzmann's constant.

I_{eq} is related to the actual diode bias current I by the derived expression^[17]

$$I_{eq} = I \coth \frac{qV}{2KT} \quad (28)$$

A plot of I_{eq} for our example diode is shown in Fig. 9, where it will be noted that I_{eq} departs considerably from I near zero bias. At zero bias, I_{eq} must equal the value corresponding to the thermal noise of the conductance G_0 , i.e.,

$$i_{n0}^2 = 4KT G_0 B_v \quad \text{or} \quad I_{eq0} = \frac{2KT G_0}{q} \quad (29)$$

In addition to the diode noise, a practical video detector is always associated with an equivalent video circuit resistance R_v , which generates the thermal noise voltage $4KT B_v R_v$. The resistance R_v includes the bias circuit for the diode plus the input impedance of the amplifier utilized with the detector. Fig. 8(b) illustrates the midband⁵ equivalent video noise circuit, where R_v noise plus diode noise contributions have been lumped into the equivalent noise current generator, $I_n^2 \cdot I_n^2$ will be equal to,

$$I_n^2 = \frac{2qI_{eq} B_v}{(1 + GR_s)^2} + \frac{4KT B_v R_s}{(R + R_s)^2} + \frac{4KT B_v}{R_v} \quad (30)$$

The output noise voltage E_n^2 produced by I_n^2 is therefore

$$E_n^2 = I_n^2 R_i^2 \quad (31)$$

where

$$R_i = \left(\frac{R_v (R_s + R)}{R_v + R_s + R} \right) \quad (32)$$

R_i is the total equivalent resistance, being the parallel combination of R_v and $(R_s + R)$. It should be pointed out that (32) is particularly significant for a tunnel-diode detector because of the fact that R can become large and, also, may be negative. Either condition will restrict the maximum value that R_v can take. For instance, the stability criteria for the video circuit require that R_i be positive, so that from (32)

⁵ "Midband" refers to the middle of the video passband determined by the video amplifier.

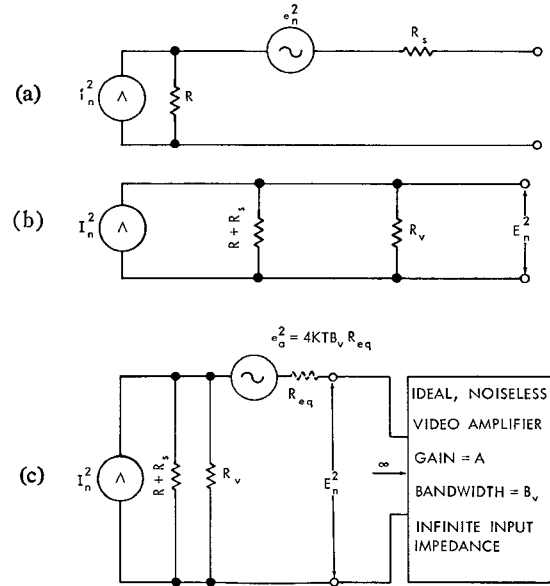


Fig. 8. Equivalent video noise circuits (midband). (a) Tunnel diode alone. (b) Tunnel diode plus video circuit resistance R_v . (c) Tunnel diode plus R_v plus excess amplifier noise e_a^2 .

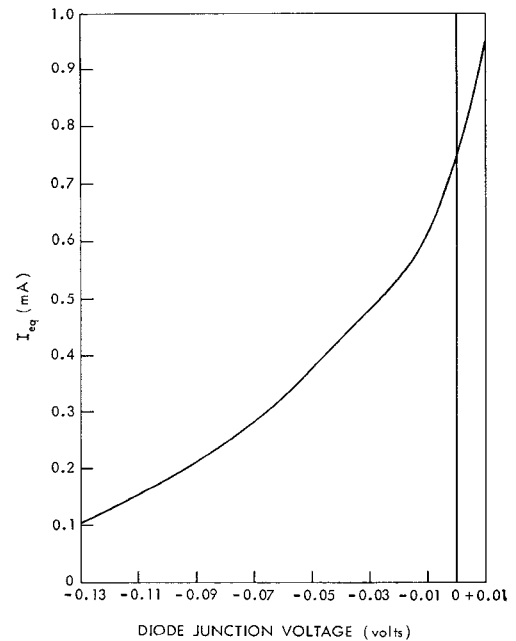


Fig. 9. Equivalent shot noise current versus junction voltage for example diode.

one obtains the necessary condition that

$$R_v < |R_s + R| \quad \text{for negative } R. \quad (33)$$

Furthermore, it may be necessary to place an upper bound upon R_i in order to obtain sufficient video bandwidth, and this upper bound on R_i will, in turn, restrict the maximum value that R_v may have.

Amplifier excess noise, which is always present in high-sensitivity video detection, can be represented by placing an equivalent noise generating resistance^{[1], [40]} R_{eq} between the detector video circuit and an ideal amplifier with an

infinite input impedance as shown in Fig. 8(c). The total noise voltage E_n^2 therefore has e_a^2 added to (31), becoming

$$E_n^2 = I_n^2 R_i^2 + 4KTB_v R_{eq} \quad (34)$$

Values of R_{eq} are readily determined from measurements of the amplifier gain, bandwidth, and rms output noise under known input circuit conditions.

Video noise bandwidth has never been satisfactorily standardized and is usually different for each detector application, so that it is desirable to normalize all noise contributions in terms of noise per cycle of video bandwidth. Thus, dividing (34) and (30) by B_v we obtain,

$$\left(\frac{E_n^2}{B_v}\right) = \left(\frac{I_n^2}{B_v}\right) R_i^2 + 4KTR_{eq} \quad (35)$$

and

$$\left(\frac{I_n^2}{B_v}\right) = \frac{2qI_{eq}}{(1 + GR_s)^2} + 4KT\left(\frac{1}{R_v} + \frac{R_s}{(R + R_s)^2}\right) \quad (36)$$

A plot of $\sqrt{I_n^2/B_v}$ versus diode junction voltage for the example diode is shown in Fig. 10 under two R_v conditions: a) R_v held constant at 265 ohms for all bias voltages, and b) maximum R_v for each bias voltage subject to the restriction that $R_i \leq 1000$ ohms. The 1 k Ω upper bound chosen for R_i represents a typical design value for wideband video detector circuits, and the two R_v conditions encompass the resultant design range for R_v . For diode junction voltage above -0.04 volts, R_v can be infinite so that this segment of the lower curve (maximum R_v) in Fig. 10 represents the noise current contributed by the diode alone. The measured data points shown in Fig. 10 were obtained from rms noise voltage measurements⁶ on the example diode, and they agree with the calculated curves within the limits of experimental measurement error.

Fig. 11 illustrates the total rms noise voltage per $\text{Hz}^{1/2}$, $\sqrt{E_n^2/B_v}$, versus diode junction voltage for the same conditions utilized in Fig. 10 plus the addition of amplifier excess noise. The set of curves for $R_{eq} = 0$ gives the noise voltage that could be obtained with an ideal noiseless amplifier, and the set of curves for $R_{eq} = 1$ k Ω illustrate the noise voltage that would be obtained with a typical transistor video amplifier of recent design.

These noise curves point up several interesting features associated with tunnel-diode video detectors:

- 1) The considerable variation in noise voltage level versus diode bias reflects the variation that occurs in R_i , (32). Video resistance R_v affects the shape and peak value of the R_i variation.
- 2) In the vicinity of zero bias where R_i becomes less than 100 ohms, amplifier noise can easily dominate the diode noise and thus degrade sensitivity.

⁶ The video amplifier utilized in conducting the noise measurements on the example diode had the following characteristics: gain, 10 000; bandwidth, 2 mHz; input impedance, 50 k Ω and 60 pF; noise R_{eq} 730 ohms. Noise due to R_{eq} was subtracted out in order to obtain diode noise data.

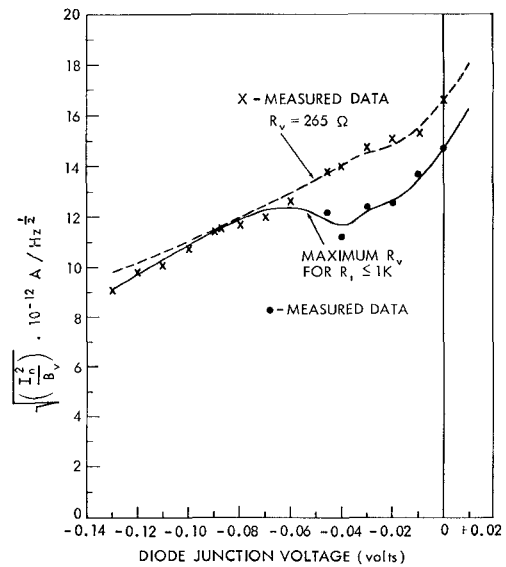


Fig. 10. $\sqrt{I_n^2/B_v}$ versus junction voltage for example diode under two R_v conditions.

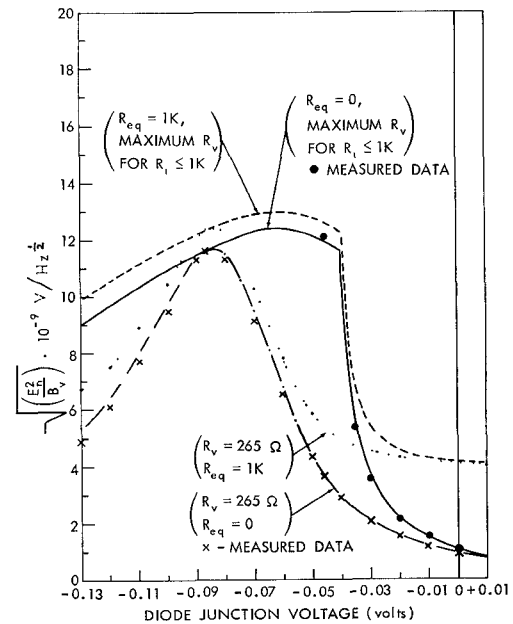


Fig. 11. $\sqrt{E_n^2/B_v}$ versus junction voltage for example diode under two R_v conditions for $R_{eq} = 0$ and $R_{eq} = 1$ k Ω .

- 3) When the diode is biased near its peak current point or beyond into the negative resistance region, R_i increases such that the diode noise becomes dominant over the amplifier noise. This latter situation is very desirable for practical high-sensitivity detection.

VI. TANGENTIAL SENSITIVITY

Tangential sensitivity^{[41],[42]} is defined as that signal level which raises the noise by its own width on an oscilloscope pulse plus noise presentation. This sensitivity criterion has the disadvantage of being somewhat dependent upon particular receiver conditions and particular observer interpretation, but it is still the most practical criterion available for measuring the sensitivity performance of low-level video

detectors. It is generally found to be consistent within ± 1 dB in RF power level for given receiver conditions and a given observer. To overcome the problem of changing receiver conditions and/or changing observers, it is necessary to measure the average signal to noise ratio actually associated with a given receiver-observer setup, and then correct the measured data to the fixed reference value of 8 dB which is utilized in the literature for calculation and comparison of tangential sensitivity performance. 8 dB results in a voltage ratio of 2.5 in the video circuit, and this value will be employed in the calculations to follow.

The minimum video detector equivalent circuit⁷ needed for computing tangential sensitivity is shown in Fig. 12. It consists of the midband video equivalent noise circuit discussed in the preceding section, plus the rectification current generator I_r and the total shunt capacitance C_v . Shunt capacitance includes the amplifier input capacitance, the detector RF bypass condenser, and shielded cable capacitance, if present. The presence of C_v places an upper bound on the values that R_i may have because of bandwidth considerations. The bandwidth of the circuit must be adequate for the pulse response required and, in addition, it is always desirable to have the input circuit bandwidth exceed the amplifier bandwidth in order to minimize amplifier noise contribution. The 3 dB bandwidth point will occur when $\omega R_i C_v = 1$, so that we require

$$R_i < \frac{1}{2\pi C_v B_v} \quad (37)$$

This upper bound on R_i may also be expressed in terms of τ , the pulse risetime between 10 and 90 percent amplitude points, since video bandwidth and pulse risetime have the approximate product^{14,31}

$$\tau B_v \approx 0.35 \quad (38)$$

so that

$$R_i < \frac{\tau}{2.2 C_v} \quad (39)$$

This restriction upon R_i results in a restriction upon the maximum value of R_v via (32), i.e., from (32) we get

$$R_v = \left[\frac{R_i}{1 - \frac{R_i}{R_s + R}} \right] \quad (40)$$

Assuming that R_i is adjusted for an adequate safety margin in (37), then the voltage E_s developed is simply

$$E_s = I_r R_i = \beta P_i R_i \quad (41)$$

⁷ The terminology "minimum circuit" is used in the sense that there can never be fewer components than shown in Fig. 12. Needless to say, actual detector video circuits are oftentimes considerably more complicated due to the presence of chokes, transformers, pulse peaking circuits, etc.

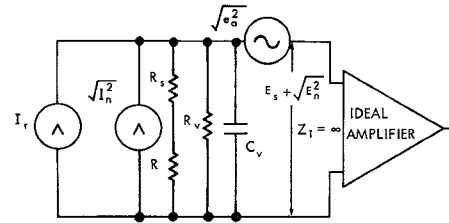


Fig. 12. Minimum video equivalent circuit.

where βP_i has been substituted for the rectification current from (6). The tangential sensitivity ratio, then, defines a particular input RF power level, $P_i = P_t$, such that the 8 dB ratio of E_s to $\sqrt{E_n^2}$ is obtained

$$\frac{E_s}{\sqrt{E_n^2}} = 2.5 = \frac{\beta R_i P_t}{\sqrt{B_v} \cdot \sqrt{\left(\frac{I_n^2}{B_v}\right) R_i^2 + 4KTR_{eq}}} \quad (42)$$

or

$$P_t = \left(\frac{2.5\sqrt{B_v}}{\beta}\right) \sqrt{\left(\frac{I_n^2}{B_v}\right) + \left(\frac{4KTR_{eq}}{R_i^2}\right)} \quad (43)$$

Note that when the amplifier noise contribution becomes negligible, (43) simplifies to

$$P_t = 2.5 \frac{I_n}{\beta} \quad (44)$$

Equation (44) can be plotted versus frequency for our example diode by utilizing values of β from Fig. 5 and values of $\sqrt{I_n^2/B_v}$ from Fig. 10. The resultant tangential sensitivities are shown plotted in Fig. 13. The left-hand scale gives $P_t/\sqrt{B_v}$ in dBm per Hz^{1/2} and the right-hand scale gives P_t in dBm for a video noise bandwidth of 1 mHz. The comments which were made on the β curves of Fig. 5 would apply equally well to Fig. 13, since there is only a small relative shift in the curves caused by the change in noise current with bias voltage. In addition, it will be noted that the tangential sensitivities that can be achieved at frequencies below f_r are at least an order of magnitude better than the performance of other types of diodes.¹¹⁻¹³

The calculated curves of Fig. 13 have been experimentally verified with the example diode at frequencies of 3, 5, 6, and 7 GHz, as illustrated by the data points plotted thereon.

The experimental receiver setup for measuring tangential sensitivity had a consistent value of 4 for the ratio of observer interpreted peak to peak noise amplitude on the oscilloscope as compared to the measured rms value. This results in a tangential sensitivity signal to noise ratio of 12 dB on the video side for the experimental measurements. Since the calculated curves are based upon the fixed reference value of 8 dB, all experimental data was corrected by the square root of the difference, or 2 dB, in order to obtain a valid compari-

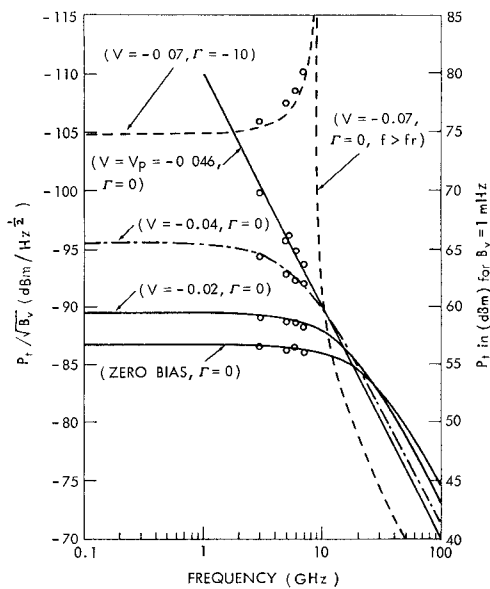


Fig. 13. Tangential sensitivity versus frequency for example diode under conditions of $R_i \leq 1\text{k}\Omega$ and $R_{eq} = 0$.

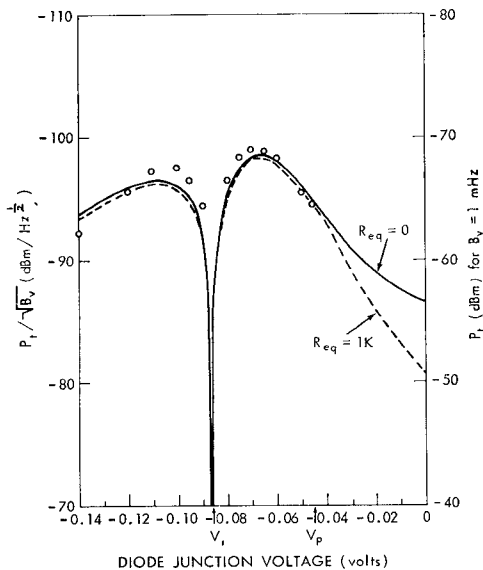


Fig. 14. Tangential sensitivity versus junction voltage for example diode under conditions of $R_i \leq 1\text{k}\Omega$ and R_{eq} either zero or $1\text{k}\Omega$.

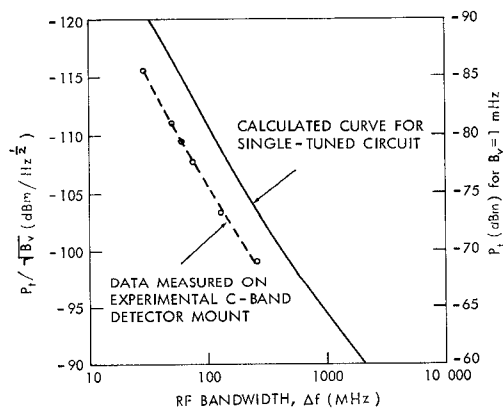


Fig. 15. Tangential sensitivity versus RF bandwidth for example diode under conditions of $V = -0.07$ volts and circuit resonance at 6GHz .

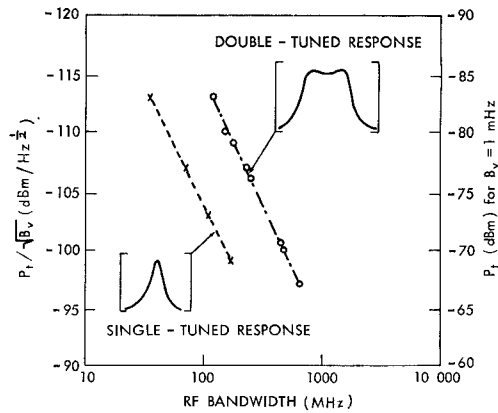


Fig. 16. Experimental comparison between single-tuned response and double-tuned response. MS1202 diode at 6GHz .

son with the calculated curves. (The square root of the 4 dB difference must be taken because low-level detection is square law and the video difference must be referred to the RF side of the detector.)

A typical variation in tangential sensitivity versus bias for the example diode is shown in Fig. 14, calculated by utilizing values of β from Fig. 6(a) and values of $\sqrt{E_n^2/B_v}$ from Fig. 11 with maximum R_v for $R_i \leq 1\text{k}\Omega$ and amplifier noise R_{eq} either zero or $1\text{k}\Omega$ as denoted on the curves. It will be noted that amplifier noise reduces tangential sensitivity significantly in the vicinity of zero bias, but becomes negligible when the diode is biased near the peak current point or beyond. Sensitivity drops to zero very sharply at the inflection point where β goes through zero [see Fig. 6(a)]. The highest peak tangential sensitivity point is readily determined via bias adjustment.

A typical variation in tangential sensitivity versus RF bandwidth for the example diode is shown in Fig. 15, calculated by utilizing values of β and Δf from Fig. 7 which were determined on the assumption of fixed element, single-tuned circuit behavior. The associated noise current was obtained from Fig. 10 for an operating bias point of -0.07 volts. Fig. 15 also contains a plot of P_t versus Δf as measured on the example diode in a tuned C-band detector mount. This particular mount did not have a bandwidth performance equal to that of a fixed-element single-tuned circuit because of the frequency dependence of R_q and L . Since the tangential sensitivity variations mainly reflect the variations that occur in β , the bandwidth comments in Section IV apply directly here.

An example of the increased bandwidth that can be obtained from more complex circuit design is shown in Fig. 16, where the performance of a double-tuned response design is compared with a single-tuned response design. It will be noted that the bandwidth was improved by a factor of three in this particular instance.

As a practical note, it might be pointed out that a P_t versus Δf plot provides a very effective means for evaluating the relative performance of tunnel diodes when measured in the same detector mount at the same resonant frequency.

VII. FIGURE OF MERIT, COMPARISON WITH HOT CARRIER DIODE

The figure of merit M which is often utilized as a criterion of excellence for video detectors, is defined as^[1]

$$M = \frac{\sqrt{4KT B_v} E_s}{P_i \sqrt{E_n^2}} \quad (45)$$

Substituting (41) for E_s and (34) for E_n^2 , one obtains

$$M = \frac{\beta}{\sqrt{\frac{I_n^2}{4KT B_v} + \left(\frac{R_{eq}}{R_i}\right)^2}} \quad (46)$$

Utilizing values of β from Fig. 6(a) and noise current from Fig. 10, substitution into (46) results in a typical figure of merit plot versus junction voltage shown in Fig. 17 for amplifier noise R_{eq} of zero and 1 k Ω . Important points to note are that when the diode is biased into the negative resistance region, amplifier noise is no longer significant and figures of merit in the thousands are readily achieved.

The figure of merit criterion offers the best means for comparing the relative sensitivity performance of a tunnel diode against a hot carrier diode. For the purposes of this comparison it is reasonable to neglect amplifier noise, i.e., let $R_{eq}=0$ so that (46) simplifies to

$$M = \frac{\beta}{\sqrt{\frac{I_n^2}{4KT B_v}}} \quad (47)$$

For the tunnel diode, values of β are calculated from (16), (18), or (19) depending upon whether G is positive, zero, or negative, and the noise current is calculated from (30).

For the hot carrier diode, values of β are calculated only from (16) since G is always positive. The noise current may be approximated by the thermal conductance noise,^[3] since this is a unique low-noise property of the diode if the video bandwidth lies above the flicker noise corner frequency. For the hot carrier diode

$$I_n^2 \approx \frac{4KT B_v}{R_s + R} \quad (48)$$

Upon substituting (16) and (48) into (47) and assuming optimum performance ($\Gamma=0$), the figure of merit for a hot carrier diode, denoted as M_{hc} , becomes

$$M_{hc} = \frac{\beta_0 \sqrt{R_s + R}}{\left[1 + \left(\frac{f}{f_c}\right)^2\right]} \quad (49)$$

β_0 is particularly simple for a hot carrier diode because the ratio of G and its first derivative remains constant, i.e., the diode current may be written as^[2]

$$I = I_s(e^{\alpha V} - 1) \quad (50)$$

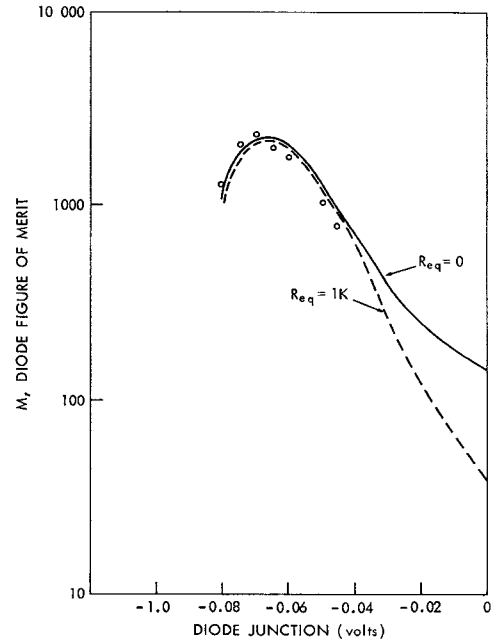


Fig. 17. Figure of merit M versus junction voltage for example diode under conditions of $R_s=85$ ohms, and detector circuit resonance at 3 GHz.

where

$$\alpha = \frac{qV}{nKT} \approx 38,$$

I_s = saturation current, and

V = diode junction voltage.

Then

$$G = \frac{dI}{dV} = \alpha I_s e^{\alpha V} \quad (51)$$

and

$$G' = \frac{dG}{dV} = \alpha^2 I_s e^{\alpha V}. \quad (52)$$

Thus, the ratio of G' to G is equal to α and substitution into (15) gives for the hot carrier diode

$$\beta_0 = \frac{\alpha}{2(1 + GR_s)^2} \approx \frac{19}{(1 + GR_s)^2} \quad (53)$$

Upon substituting this β_0 into (49) and simplifying, M_{hc} becomes

$$M_{hc} \approx \frac{19\sqrt{R}}{(1 + GR_s)^{3/2} \left[1 + \left(\frac{f}{f_c}\right)^2\right]} = \frac{M_{hc0}}{\left[1 + \left(\frac{f}{f_c}\right)^2\right]} \quad (54)$$

where f_c is given by (17).

For calculation, the published characteristics of typical hpa-2350 diodes^[3] were utilized: series resistance $R_s \approx 12$ ohms, junction capacitance $C \approx 0.75$ pF, and $I_s = 8 \cdot 10^{-9}$ amperes. The figure of merit performance for this particular hot carrier diode is illustrated by the dashed-line curves in

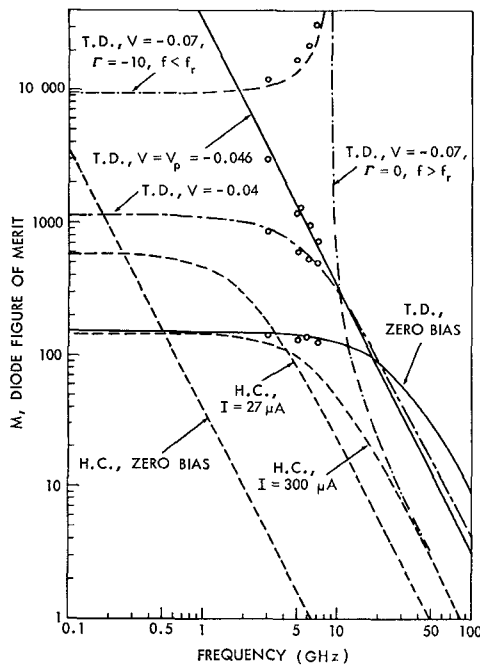


Fig. 18. Figure of merit M versus frequency for example diode and a hot carrier diode hpa-2350 under various bias conditions.

Fig. 18 for three bias conditions; zero bias, $I = 27 \mu\text{A}$, and $I = 300 \mu\text{A}$. These calculated curves are found to be in close agreement with the published tangential sensitivity data for the diode^[3] when cross checked via the relationship derived from (45),

$$\left(\frac{\sqrt{B_v}}{P_t}\right) = \frac{M}{2.5\sqrt{4KT}} = 3.16 \cdot 10^9 M. \quad (55)$$

The curves clearly illustrate the trade-off between $M_{h.c.0}$ and f_c as the bias current I is increased.

The example diode was utilized for calculating the tunnel-diode performance as illustrated by the lines labelled "T.D." in Fig. 18 for four junction voltage conditions; zero bias, $V = -0.04$ volts, $V = V_p$, and $V = -0.07$ volts. Some experimental confirmation data points are included. It will be noted that the tunnel diode has a better sensitivity capability than the hot carrier diode for the examples shown here, even when the tunnel diode is restricted to positive conductance biasing. When biased to V_p or beyond into the negative resistance region, as illustrated by the broken line curve for $V = -0.07$ volts, the tunnel diode is capable of at least an order of magnitude improvement in sensitivity over the hot carrier diode for frequencies below f_r .

VIII. CONCLUSIONS

A low-level detection analysis of the tunnel diode has been presented with the aim of covering its detection behavior for any bias condition, particularly in the negative resistance region. It has been shown that for negative resistance biasing, the tunnel diode exhibits the following interesting detection properties:

1) For a bias excursion through the inflection point, the detector shows a discriminator-like rectification reversal

behavior, with the zero output point anchored precisely at the inflection bias point.

2) For frequencies below resistive cutoff, sensitivity is proportional to $(1 - \Gamma^2)$, where Γ^2 is the RF power gain of the detector viewed as a reflection-type amplifier, so that unusually high sensitivities can be achieved.

3) For frequencies above resistive cutoff, the sensitivity drops rather abruptly and quickly becomes inferior to the zero bias sensitivity.

The unusually high sensitivities which are made possible via control of Γ^2 must necessarily be subject to all of the trade-offs that are associated with high-gain RF amplifiers, and it was shown that the usual gain bandwidth product applies directly, i.e., a higher sensitivity can only be achieved at the expense of a smaller bandwidth. Other trade-offs, familiar to the tunnel-diode amplifier art, include greater temperature variation, more critical bias regulation, a lower saturation power level, and more critical circuit stability conditions. If one is willing to accept the trade-offs, then sensitivities an order of magnitude better than any other video detector are readily achieved. In fact, the sensitivity can actually be pushed to the point of being competitive with a superheterodyne receiver under certain conditions.

A practical by-product of this detection study was the observation that the rectified current from a tunnel-diode amplifier provides a very sensitive and valuable tool during the design and adjustment phase of an amplifier, since it can be utilized to monitor bias stability, spurious oscillation, band-pass shape, bandwidth adjustment, temperature effects, saturation effects, extraneous signals, etc. The rectified current could also be incorporated into a feedback loop for bias point control or automatic gain control.

Special mention must be made of the peak current bias point of a tunnel diode. It was shown that this particular bias point results in a sensitivity inversely proportional to the square of the frequency, and this behavior results in unusually high sensitivities at the lower microwave frequencies. The easy stability conditions involved in peak current biasing make it a very attractive operating point.

APPENDIX I

DERIVATION OF β

The rectification current sensitivity β is given by the ratio of I_r to P_i ,

$$\beta = \frac{I_r}{P_i}. \quad (56)$$

By restricting P_i to low levels such that the RF voltage excursion on the nonlinear diode characteristic is small compared to the radius of curvature, then Taylor series approximations^[4] can be employed to derive an accurate expression for low-level rectification.

The equivalent RF circuit shown in Fig. 1 of the main text will be utilized for this analysis, but it requires the addition of a zero impedance bias battery V_b , in series with the RF generator E_θ , in order to represent the dc bias voltage applied across the diode.

Fig. 19 illustrates a nominal nonlinear junction characteristic. Since the excursions about the bias point are assumed to be very small, it is permissible to express the nonlinear current I as a Taylor series expansion of three terms about the bias point

$$I = f(V_{jb} + v) \approx f(V_{jb}) + f'(V_{jb}) \cdot v + \frac{1}{2} f''(V_{jb}) \cdot v^2 + \dots \quad (57)$$

where v is the excursion of V about the junction bias voltage V_{jb} , i.e.,

$$v = V - V_{jb}. \quad (58)$$

The first term, $f(V_{jb})$, is simply the bias current I_b . The second term is the linear RF current determined by the differential junction conductance G at the bias point

$$f'(V_{jb}) = \left(\frac{dI}{dV} \right)_{V=V_{jb}} = G. \quad (59)$$

In the third term, the second derivative of the function may also be written as the first derivative of the conductance, i.e.,

$$f''(V_{jb}) = \left(\frac{d^2I}{dV^2} \right)_{V=V_{jb}} = \left(\frac{dG}{dV} \right)_{V=V_{jb}} = G'. \quad (60)$$

Thus, (57) may be written

$$I \approx I_b + Gv + \frac{1}{2} G'v^2. \quad (61)$$

The current I may now be combined with the current through the condenser, Cdv/dt , to give the current I_o , i.e.,

$$I_o = I + C \frac{dv}{dt} \approx I_b + Gv + C \frac{dv}{dt} + \frac{1}{2} G'v^2. \quad (62)$$

Voltage V must be related to the applied RF signal E_g which is assumed to be a small sinusoid

$$E_g = be^{j\omega t}, \quad b \ll V_b. \quad (63)$$

The necessary relationship may be established by writing I_o as a Taylor series expansion in terms of the applied voltages ($V_b + E_g$), whereupon one obtains by inspection

$$I_o \approx I_b + \frac{E_g}{Z} + I_r \quad (64)$$

where I_r is the rectified current and Z is the total series impedance of the circuit. Utilizing this approximation for I_o , it follows that the voltage V across the diode junction is given by

$$V \approx V_b - R_s(I_b + I_r) + \frac{Z_j}{Z} \cdot E_g \quad (65)$$

where Z_j is the equivalent series impedance of the diode junction

$$Z_j = \left(\frac{1}{G + j\omega C} \right). \quad (66)$$

R_g does not enter into the dc voltage drop in (65) because the detector mount is assumed to have a dc current return.

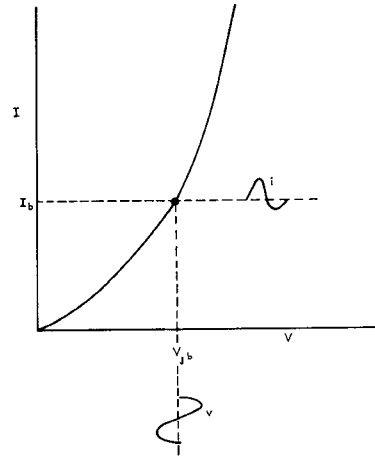


Fig. 19. Nominal V - I characteristic illustration.

Since $V_{jb} = V_b - R_s I_b$, then (58) and (65) result in the desired relationship

$$v = V - V_{jb} \approx \left(\frac{Z_j}{Z} \right) E_g - R_s I_r. \quad (67)$$

Substituting this expression for v into (62) permits writing I_o in the form

$$I_o \approx I_b - GR_s I_r + \frac{E_g}{Z} + \frac{1}{2} G' \left[b \left| \frac{Z_j}{Z} \right| e^{j(\omega t + \theta)} - R_s I_r \right]^2. \quad (68)$$

Upon equating this I_o to the I_o found in (64), the I_b term and the linear E_g/Z term will drop out, leaving

$$I_r \approx -GR_s I_r + \frac{1}{2} G' \left[b \left| \frac{Z_j}{Z} \right| e^{j(\omega t + \theta)} - R_s I_r \right]^2. \quad (69)$$

Only the average value of the squared term is of interest so that it is necessary to take the real part thereof. Furthermore, the voltage drop ($R_s I_r$) is very small compared to the RF magnitude of v , i.e.,

$$b \left| \frac{Z_j}{Z} \right| \gg R_s I_r. \quad (70)$$

Therefore, $R_s I_r$ can be neglected in the squared term and (69) becomes

$$I_r(1 + GR_s) \approx \frac{1}{2} G' \left[b \left| \frac{Z_j}{Z} \right| \cos(\omega t + \theta) \right]^2 \quad (71)$$

from which the average value is obtained to arrive at the rectified current

$$I_r \approx \frac{G' b^2 |Z_j|^2}{4(1 + GR_s) |Z|^2}. \quad (72)$$

In Fig. 1, if the resistance R_g is derived entirely from the generator source impedance,⁸ then the incident RF power may be expressed in terms of E_g as

$$P_i = \frac{1}{2} \cdot \frac{|E_g|^2}{4R_g} = \frac{b^2}{8R_g}. \quad (73)$$

Upon dividing (72) by (73), the expression for the rectification current sensitivity β is obtained,

$$\beta = \frac{I_r}{P_i} \approx \frac{2G'R_g |Z_j|^2}{(1 + GR_s) |Z|^2}. \quad (74)$$

APPENDIX II

TUNNEL-DIODE V - I CHARACTERISTIC

The voltage-current characteristic of a tunnel diode has not been rigorously derived as yet, so that no single equation is known that is capable of accurately predicting the entire curve.^{[16]-[17]} However, a reasonably accurate piecewise approximation can be obtained by curve-fitting with an exponential function of the type derived in Nergaard and Glicksman^[15] for an assumed tunnel-diode model

$$I = 2.44I_p(\alpha V)^{1.5}e^{\alpha V} \quad (75)$$

where

$$\alpha = \frac{q}{KT} = \frac{1.6 \cdot 10^{-19} \text{ coulombs}}{4 \cdot 10^{-21} \text{ W/HZ}},$$

I_p = peak current, and

V = voltage across diode junction.

For curve-fitting, it is desirable to utilize the general form of (75), together with its first two derivatives,

$$I = A(\alpha V)^{\gamma}e^{\alpha V} \quad (76)$$

$$\frac{dI}{dV} = I \left(\frac{\gamma}{V} + \alpha \right) = G \quad (77)$$

$$\frac{d^2I}{dV^2} = I \left[\alpha^2 + \frac{2\alpha\gamma}{V} + \frac{\gamma(\gamma - 1)}{V^2} \right] = G'. \quad (78)$$

It will be noted in (77) that the first derivative is the junction conductance G of the diode, and in (78) that the second derivative is therefore G' .

The above relationships apply only to the diode junction, so that it is necessary to add a fourth equation in order to account for the series resistance R_s ,

$$V_b = V + IR_s \quad (79)$$

where V_b now represents the external voltage across the diode terminals. The value of R_s must be known accurately not only because of its effect upon the V - I characteristic, but also because of its effect upon the microwave performance of the diode. R_s is usually provided as part of the manufacturer's data on the diode, but if it is not known or is in ques-

tion then it may be determined from I - V_b slope measurements under forward bias conditions. The necessary relationship is readily obtained by differentiating (79)

$$\frac{dV_b}{dI} = \frac{dV}{dI} + R_s = \frac{1}{\left(\frac{dI}{dV}\right)} + R_s. \quad (80)$$

Substituting for (dI/dV) from (77) then results in

$$\frac{dV_b}{dI} = \frac{1}{\left(\frac{\gamma}{V} + \alpha\right)} \cdot \left(\frac{1}{I}\right) + R_s. \quad (81)$$

If the forward bias voltage is large enough to obtain the condition $\gamma/V \ll \alpha$, then (81) simplifies to

$$\frac{dV_b}{dI} = \frac{1}{\alpha I} + R_s \quad (82)$$

which is a straight line graph of (dV_b/dI) versus $(1/I)$ with R_s given by the intersection of the straight line with the (dV_b/dI) axis.

In curve-fitting the forward characteristic of the diode, it has been found that satisfactory accuracy may be obtained by utilizing the I - V_b slope measured at zero bias, plus the reverse bias peak current point values of I_p , V_{bp} . The zero bias slope G_{d0} is finite and requires a current component I_1 , for which the value of γ in (76) is unity,

$$I_1 = A_1(\alpha_1 V)e^{\alpha_1 V} \quad (83)$$

$$\frac{dI_1}{dV} = G_1 = A_1\alpha_1 e^{\alpha_1 V} + \alpha_1 I_1 \quad (84)$$

$$\left. \frac{dI_1}{dV} \right|_{V=0} = G_0 = A_1\alpha_1. \quad (85)$$

At the peak current point, G_1 must go to zero so that from (83) and (84) we obtain

$$\left. \frac{dI_1}{dV} \right|_{V=V_p} = 0 = I_{p1} \left(\frac{1}{V_p} + \alpha_1 \right)$$

or

$$\alpha_1 = \frac{1}{-V_p}. \quad (86)$$

V_p can be obtained from (79),

$$V_p = V_{bp} - I_p R_s \quad (87)$$

so that α_1 is determined. Then A_1 is evaluated from (85). Utilizing the MS1012 diode as an example, the following values were measured:

$$R_s = 8 \text{ ohms}, \quad I_p = -0.285 \text{ mA},$$

$$V_{bp} = -0.0483 \text{ volts}, \quad G_{d0} = 0.0133 \text{ mhos.}$$

⁸ If R_s includes resistance other than from the generator, then a loss correction must be calculated.

From this data, the values of α_1 and A_1 were calculated and found to be 21.75 V^{-1} and 0.687 mA , respectively.

The resulting I_1 equation was found to hold within 4 percent of the measured data for forward bias up to 40 mV and for reverse bias to about -8 mV . Values of G and G' were calculated from I_1 within this voltage range.

A single equation curve fit of the negative characteristic is best accomplished by utilizing the inflection point data together with V_p . At the inflection point the second derivative must vanish, so that from (78) one obtains

$$\left. \frac{d^2 I}{dV^2} \right|_{V=V_i} = \alpha^2 I_i \left[1 + \frac{2\gamma}{\alpha V_i} + \frac{\gamma(\gamma-1)}{(\alpha V_i)^2} \right] = 0 \quad (88)$$

which has the solution

$$\alpha V_i = -(\gamma + \sqrt{\gamma}). \quad (89)$$

Upon substituting the peak current condition obtained from setting (77) equal to zero

$$\left. \frac{dI}{dV} \right|_{V=V_p} = 0 = I_p \left[\frac{\gamma}{V_p} + \alpha \right] \quad (90)$$

or

$$\alpha = \frac{\gamma}{-V_p}. \quad (91)$$

Then (89) may be written as

$$V_i = V_p \left(1 + \frac{1}{\sqrt{\gamma}} \right). \quad (92)$$

By substituting (92) and (91) into (76) one can relate the inflection point current to the peak current

$$I_i = \frac{\left(1 + \frac{1}{\sqrt{\gamma}} \right)^\gamma}{e^{\sqrt{\gamma}}} \cdot I_p. \quad (93)$$

The final relationship needed is the slope (conductance) at the inflection point, and this is obtained by substituting (92), (93), and (91) into (77)

$$G_i = I_i \left(\frac{\gamma}{V_i} + \alpha \right) = - \frac{\gamma^{1-\gamma/2} (1 + \sqrt{\gamma})^{\gamma-1}}{e^{\sqrt{\gamma}}} \cdot \frac{I_p}{V_p}, \quad (94)$$

which may then be written as

$$- \frac{\gamma^{1-\gamma/2} (1 + \sqrt{\gamma})^{\gamma-1}}{e^{\sqrt{\gamma}}} = \left(\frac{V_p}{I_p R_i} \right) \quad (95)$$

where R_i is the inflection point negative resistance.

Equation (95) results in the ratio of V_p to $I_p R_i$ as a function of γ only. In curve-fitting to the actual diode characteristic, only three of the five conditions (I_p , V_p , I_i , V_i , R_i) can be satisfied by the three constants available to us in the single equation (76), so that the remaining two quantities

must be compromised. In practice, it has been found that the most satisfactory compromise is obtained by using the measured values of V_p and R_i , and choosing the inflection point to lie on the measured data curve. This throws most of the compromise error into the magnitude of I_p , but the price paid is small. Again utilizing the MS1012 diode as an example, the measured data for V_p and R_i was -0.046 volts and -368 ohms , respectively. The best curve fit at the inflection point occurred for a value of $\gamma = 1.275$. Having determined the value of γ , one can then calculate that the constant $\alpha_2 = 27.73 \text{ V}^{-1}$, and $A_2 = 0.755 \text{ mA}$ to complete the equation for I_2 ,

$$I_2 = A_2 (\alpha_2 V)^\gamma e^{\alpha_2 V}. \quad (96)$$

The I_2 piecewise current approximation held within 4 percent accuracy for reverse bias voltage range of -20 to -130 mV in this particular case.

APPENDIX III

LIST OF SYMBOLS AND DEFINITIONS

- A —constant in diode current equation, Appendix II
- b —amplitude of E_g
- B_v —video bandwidth
- C —diode junction capacitance
- C_b —RF bypass condenser
- C_v —total video shunt capacitance
- C_p —diode package and mounting capacitance
- E_g —series equivalent RF signal generator voltage
- $\sqrt{E_n^2}$ —total rms noise voltage
- f —RF frequency
- f_c —diode cutoff frequency for positive R
- f_r —diode resistive cutoff frequency for negative R
- Δf —RF bandwidth
- G —diode differential junction conductance, (dI/dV)
- G' —first derivative of G
- I —resistive component of diode junction current
- I_b —diode dc bias current
- I_g —total diode current, $[I_g = I + C(dV/dt)]$
- I_p —tunnel-diode peak point current value
- I_i —tunnel-diode inflection point current value
- I_r —detector rectified output current
- I_{eq} —equivalent shot-noise-producing dc current
- $\sqrt{I_n^2}$ —total rms noise current due to diode and R_v
- K —Boltzmann's constant, $(1.38 \cdot 10^{-16} \text{ ergs per degree Kelvin})$
- L —equivalent RF circuit series inductance plus L_s
- L_s —diode series inductance
- M —diode figure of merit
- P_i —RF power incident upon the detector
- P_t —tangential sensitivity input RF power level
- q —electronic charge, $(1.6 \cdot 10^{-20} \text{ coulombs})$
- Q —circuit Q factor
- R —diode differential junction resistance, (dV/dI)
- R_g —equivalent series resistance of RF circuit
- R_s —diode series resistance
- R_v —equivalent video circuit resistance

- R_i —total equivalent resistance of diode in parallel with R_o (Note: R_i is also used in Appendix II to denote the inflection point negative resistance value of R)
- R_{eq} —amplifier excess noise equivalent resistor
- r —series equivalent junction resistance of diode
- r_0 —value of r at ω_0
- T —temperature in degrees Kelvin
- V —diode junction voltage
- V_b —diode dc bias voltage
- V_{jb} —junction dc bias voltage, ($V_{jb} = V_b - I_b R_s$)
- v —excursion of V from V_{jb} , ($v = V - V_{jb}$)
- Z —total equivalent series impedance of diode plus RF circuit
- Z_j —equivalent series impedance of diode junction
- α —constant in diode current equation, Appendix II
- β —rectification current sensitivity
- γ —constant in diode current equation, Appendix II
- Γ —reflection coefficient referred to R_o
- τ —pulse risetime between 10 and 90 percent amplitude points
- ω —frequency in radians per second
- ω_0 —value of ω at center of RF passband

Subscripts

- 0 refers to diode zero bias point except for r_0 , ω_0 , β_0 , and Γ_0
- p refers to diode peak current bias point
- i refers to diode inflection bias point except for special case noted for R_i .

REFERENCES

- [1] Torrey and Whitmer, *Crystal Rectifiers*, M.I.T. Rad. Lab. Ser., vol. 15. New York: McGraw-Hill, 1948, ch. 11.
- [2] R. N. Hall, "Design of the hot carrier mixer and detector," *IEEE Internat'l Solid-State Circuits Conf. Digest*, vol. 7, pp. 98–99, February 1965.
- [3] H. O. Sorensen, "Using the hot carrier diode as a detector," *Hewlett-Packard J.*, vol. 17, no. 4, December 1965.
- [4] S. T. Eng, "Low-noise properties of microwave backward diodes," *IRE Trans. Microwave Theory and Techniques*, vol. MTT-9, pp. 419–425, September 1961.
- [5] M. D. Montgomery, "The tunnel diode as a highly sensitive microwave detector," *Proc. IRE (Correspondence)*, vol. 49, pp. 826–827, April 1961.
- [6] J. Reindel, "The tunnel diode as a CW detector," *Proc. IEEE (Correspondence)*, vol. 51, pp. 1677–1678, November 1963.
- [7] P. E. Chase and K. K. N. Chang, "Tunnel diodes as millimeter wave detectors and mixers," *IEEE Trans. Microwave Theory and Techniques (Correspondence)*, vol. MTT-11, pp. 560–561, November 1963.
- [8] W. F. Gabriel, "The versatile tunnel-diode video detector," *IEEE Internat'l PTG-MTT Symp. Digest*, pp. 157–162, May 1964.
- [9] R. O. Wright and R. L. Goldman, "Aluminum alloy junction backward diodes in microwave detection systems," *IEEE Internat'l Solid-State Circuits Conf. Digest*, vol. 8, pp. 100–101, February 1965.
- [10] R. B. Mouw and F. M. Schumacher, "Tunnel-diode detectors," *Microwave J.*, vol. 9, pp. 27–36, January 1966.
- [11] Van Voorhis, *Microwave Receivers*, M.I.T. Rad. Lab. Ser., vol. 23. New York: McGraw-Hill, 1948, ch. 19.
- [12] H. Klipper, "Sensitivity of crystal video receivers with R.F. pre-amplification," *Microwave J.*, vol. 8, pp. 85–92, August 1965.
- [13] M. E. Hines, "High-frequency negative resistance circuit principles for Esaki diode applications," *Bell Sys. Tech. J.*, vol. 39, pp. 477–513, May 1960.
- [14] S. P. Gentile, *Basic Theory and Application of Tunnel Diodes*. Princeton, N.J.: Van Nostrand 1962.
- [15] L. S. Nergaard and M. Glicksman, *Microwave Solid-State Engineering*. Princeton, N.J.: Van Nostrand, 1964, ch. 3, 4.
- [16] K. K. N. Chang, *Parametric and Tunnel Diodes*. Englewood Cliffs, N.J.: Prentice-Hall, 1964.
- [17] W. F. Chow, *Principles of Tunnel Diode Circuits*. New York: Wiley, 1964.
- [18] L. I. Smilen and D. C. Youla, "Stability criteria for tunnel diodes," *Proc. IRE (Correspondence)*, vol. 49, pp. 1206–1207, July 1961.
- [19] L. A. Davidson, "Optimum stability criterion for tunnel diodes shunted by resistance and capacitance," *Proc. IEEE (Correspondence)*, vol. 51, p. 1233, September 1963.
- [20] I. T. Frisch, "A stability criterion for tunnel diodes," *Proc. IEEE*, vol. 52, pp. 922–923, August 1964.
- [21] J. W. Bandler, "Stability and gain prediction of microwave tunnel-diode reflection amplifiers," *IEEE Trans. Microwave Theory and Techniques*, vol. MTT-13, pp. 814–819, November 1965.
- [22] H. R. Lowry et al., *Tunnel Diode Manual*, 1st ed. New York: General Electric Co., 1961.
- [23] G. L. Matthaiei, "A study of the optimum design of wideband parametric amplifiers and up-converters," *IRE Trans. Microwave Theory and Techniques*, vol. MTT-9, pp. 23–38, January 1961.
- [24] H. Seidel and G. F. Herrmann "Circuit aspects of parametric amplifiers," *IRE WESCON Rec.*, vol. 3, pt. 2—Circuit Theory, pp. 83–90, 1959.
- [25] M. Gilden and G. L. Matthaiei, "Practical design and performance of nearly optimum wideband degenerate parametric amplifiers," *IRE Trans. Microwave Theory and Techniques*, vol. MTT-9, pp. 484–490, November 1961.
- [26] J. H. Lepoff and G. J. Wheeler, "Octave bandwidth tunnel-diode amplifier," *IEEE Trans. Microwave Theory and Techniques*, vol. MTT-12, pp. 21–26, January 1964.
- [27] J. O. Scanlan and J. T. Lim, "The effect of parasitic elements on reflection type tunnel diode amplifier performance," *IEEE Trans. Microwave Theory and Techniques*, vol. MTT-13, pp. 827–836, November 1965.
- [28] W. J. Getsinger, "Prototypes for use in broadbanding reflection amplifiers," *IEEE Trans. Microwave Theory and Techniques*, vol. MTT-11, pp. 486–497, November 1963.
- [29] R. Aron, "Gain bandwidth relations in negative resistance amplifiers," *Proc. IRE (Correspondence)*, vol. 49, pp. 355–356, January 1961.
- [30] J. Hamasaki, "A low-noise and wide-band Esaki diode amplifier with a comparatively high negative conductance diode at 1.3 Gc/s," *IEEE Trans. Microwave Theory and Techniques*, vol. MTT-13, pp. 213–223, March 1965.
- [31] E. W. Sard, "Tunnel diode amplifiers with unusually large bandwidth," *Proc. IRE (Correspondence)*, vol. 48, pp. 357–358 March 1960.
- [32] J. S. Logan, "Gain vs. bandwidth limits for Esaki diode amplifiers," *Proc. IRE (Correspondence)*, vol. 49, p. 832, April 1961.
- [33] W. C. Follmer, "Low-frequency noise in backward diodes," *Proc. IRE (Correspondence)*, vol. 49, pp. 1939–1940, December 1961.
- [34] D. C. Agouridis and K. M. van Vliet, "Noise measurements on tunnel diodes," *Proc. IRE (Correspondence)*, vol. 50, pp 2121, October 1962.
- [35] M. D. Montgomery, "Excess noise in germanium and gallium arsenide Esaki diodes in the negative resistance region," *J. Appl. Phys.*, vol. 32, pp. 2408–2410, November 1961.
- [36] M. D. Burkhard and E. F. Sidor, "Tunnel diode audio-frequency noise," *Proc. IRE (Correspondence)*, vol. 50, pp. 2487–2488, December 1962.
- [37] R. A. Giblin, "Noise spectrum measurements on tunnel diodes in the frequency range 5 Kc to 10 Mc," *Electronic Engrg.*, pp. 766–769, November 1964.
- [38] J. J. Tiemann, "Shot noise in tunnel diode amplifiers," *Proc. IRE*, vol. 48, pp. 1418–1423, August 1960.
- [39] R. A. Pucel, "The equivalent noise current of Esaki diodes," *Proc. IRE (Correspondence)* vol. 49, pp. 1080–1081, June 1961.
- [40] W. A. Rheinfielder, *Design of Low-Noise Transistor Input Circuits*. New York: Hayden, 1964.
- [41] C. G. Montgomery, *Technique of Microwave Measurements*, M.I.T. Rad. Lab. Ser., vol. 2. New York: McGraw-Hill, 1947, pp. 228–229.
- [42] S. N. VanVoorhis, *Microwave Receivers*, M.I.T. Rad. Lab. Ser., vol. 23. New York: McGraw-Hill, 1947, pp. 292, 456, 505.
- [43] Valley and Vallmon, *Vacuum Tube Amplifiers*, M.I.T. Rad. Lab. Ser., vol. 18. New York: McGraw-Hill, 1948, ch. 2.